Numerical Modeling Using the Finite Element Method of the Drill-Working Tool-Rock Wall System Taking into Account the Propagation of Longitudinal Vibrations in the Sliding Crossbeam and the Movement Mechanism of Drills

Radu Daniel[1)] , Doșa Ion[2*)] , Vîlceanu Florin[3)]

[1)]University of Petrosani; 20 University Street, 332006, Petrosani, Romania
AlinRadu@upet.ro; https://orcid.org/0009-0003-4436-3700
[2*)]University of Petrosani; 20 University Street, 332006, Petrosani, Romania
IonDosa@upet.ro; https://orcid.org/0000-0003-3696-2589
[3)]University of Petrosani; 20 University Street, 332006, Petrosani, Romania
FlorinVilceanu@upet.ro; https://orcid.org/0009-0006-5653-6957

https://doi.org/10.29227/IM-2026-02-02-037

Submission date: 2026-05-06 | Review date: *2026-22-06*

Abstract

In this paper, we present a simplified model of the vibro-mechanical behavior of the drill- working tool- rock wall system, a rather complex task for any proposed model, being very difficult to reproduce accurately the real world phenomena. The difficulties in modeling this phenomenon come from the interactions of the many different variables that define the drilling process. For this reason, a series of simplifying assumptions were made, and the study was conducted using a hypothetical (but realistic) calculation examples, comparing the results obtained analytically with those obtained numerically, refining the model in the processes. Nevertheless, this model provides insight into the mechanical phenomena occurring within the system and may serve as a basis for further studies of the drilling process and the mechanical phenomena involved.

Keywords: drill-working tool-rock wall system, percutions, vibrations, finite element

1. Introduction

Modern drilling of mine holes using the drill-and-blast method is performed with percussion, rotary-percussion, or rotary drills (depending on the rock hardness), supported by manipulators mounted on mobile units on tires, tracks, or railway wheels, depending on the transport method chosen for removing the rock resulting from blasting. The drill bits are driven into the rock using various types of mechanisms, depending on the type of drill and manipulator.

In rotary-percussion drills, which are frequently used for drilling medium-hard rock, the drill bit's advance into the rock is achieved by applying a series of impacts at a constant frequency to its shank, followed by its rotation at a specific speed. This process achieves drilling during one impact and rock chipping between two successive impacts.

The drills slide on sliding rails that incorporate their feed mechanisms (Fig.1), the sliding rails being supported by manipulators that allow the drill to be moved to the elevation and in the direction of drilling the mine hole.

The theoretical and methodological background of the present study is based on previous research related to rock drilling processes, penetration rate prediction, drilling efficiency, rock cutting mechanics, and the performance assessment of drilling and excavation systems [1–7].

2. Results obtained analytically and through FEM modeling of the drill-working tool-rock system

2.1 Presentation of the drill-working tool-rock wall system, its vibration modes, and FEM modeling

Fig. 1 shows the kinematic diagram of the movement mechanism of the P-125 drill, which is used in IMP-1 and IMP-2 drilling rigs (designed and patented at the University of Petrosani) this diagram includes the drill-cutting tool-rock system that is the subject of this paper.

Fig. 1 shows: 1-pneumatic drive motor; 2, 3-two-stage gearbox; 4-coupling system; 5-gearbox housing; 6-drive sprocket; 7, 8-sprockets for chain deflection; 9, 10—chain return wheels ( ); 11—traction chain with link-plates and rollers; 12—elastic element (coil spring); 13, 19—guides; 14—P125 type rotary percussion pneumatic hammer; 15—drill bit; 16-sliding crossbar; 17-chain tensioner; 18-cylinder for securing the sliding crossbar in the rock during drilling; 20-sliding crossbar support; 21, 22-guide sleeves (intermediate supports for the drill bit).

During drilling, the drill bit, and thus the drill itself, is pressed into the rock with a force F developed by the feed mechanism, and the drill piston repeatedly applies impacts at a certain frequency to the drill bit shank.

In the study conducted, it was assumed that during drilling, the sliding crossbar is in a horizontal position and that it does not move relative to its attachment point on the manipulator arm.

The drill moves along the sliding crossbar and is held by the feed mechanism via an elastic system (coil spring) whose elastic constant is k. The drill's movement and its pressing into the rock are performed by traction components driven by a pneumatic motor via a gearbox. The pneumatic motor can be likened to a viscous damper whose viscous damping coefficient is c .

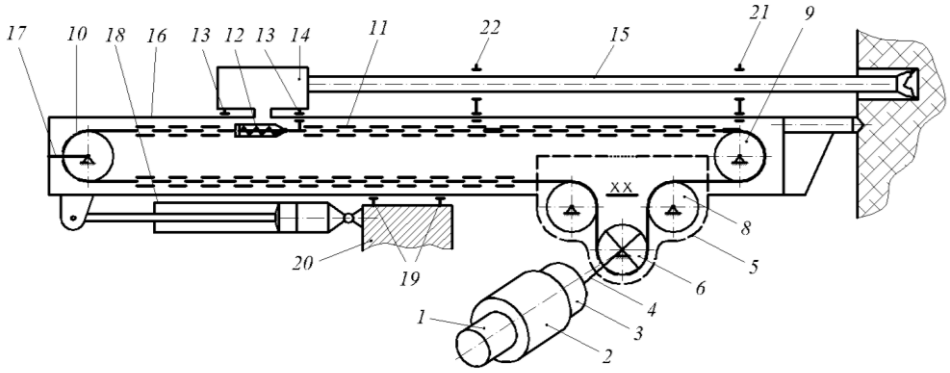

Fig. 1. Presentation of the drill-working tool-rock wall system assembly

When the rock yields at the moment of impact, the drill bit moves along the sliding crossbar a distance equal to the penetration of the drill bit's cutting edge into the rock. During the drilling process, due to the heterogeneity of the rock and the impacts applied to the drill bit, the drill has an intermittent movement, making small jumps.

When examining the longitudinal oscillations that occur during the drillbit's small jumps as the rock gives way, it is taken into account that the propagation speed of longitudinal waves is much higher than the chain's deformation speed and the linear speed of the drive sprocket's rotational motion. Taking this into account, it is considered that the drill, due to its high inertia, does not participate in such an oscillatory motion after the first jump. Therefore, it can be considered that during the displacement, the disturbing force acting on the drill becomes zero, its evolution over time is shown in Figure 2, where F_0 is the pressing force on the drill bit. It is also assumed that the constant-modulus disturbing force, F_0 , begins to act at the time $t = 0$ and ceases at $t = t_0$.

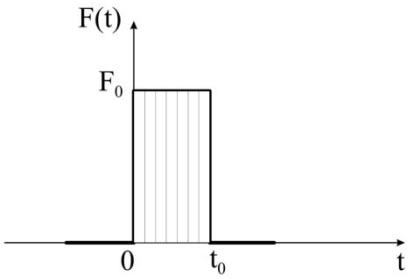

Fig. 2. Pressing force variation

Under this load, with the assumptions considered and taking into account the fact that the kick support plate guides between the two U12 profiles, which form the sliding crossbar, the kick will undergo longitudinal vibrations during the kicking process. In light of the assumptions made, an initial analysis assumes that the friction force in the guides is zero. ($F_f = 0$).

Due to the construction and operating mode described in the introduction to this paper , the drill-working tool-rock wall system can be treated as an elastic system with a single degree of freedom, with the mass undergoing translational motion.

Let us first consider the two dynamic response modes for the drill-working tool-rock wall system, specific to the vibrations of elastic systems.

a) *the case of free vibrations with viscous damping*; the dynamic model for this response mode (when there is no perturbing force ($t > t_0$) and the system oscillates around the static equilibrium position) is presented in Fig. 3.

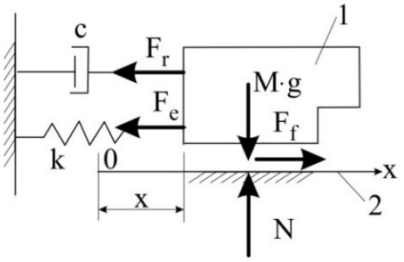

Fig. 3. Free dampening vibrations model

The following notations are used:

$F_e = -kx$ is the elastic force arising in the coil spring;

$F_r = -cx$ is the resistive force that arises in the damper;

x'', x', x are the *acceleration*, *velocity*, and *displacement* of the mass M of the hammer-drill;

k is the elastic constant of the hammer-drill;

c is the viscous damping coefficient

$\frac{c}{M} = 2\alpha$ is the damping factor

$\frac{K}{M} = \omega^2$ is the square of the amplitude

By projecting all forces onto the direction of oscillation, we obtain the differential equation:

$$M\ddot{x} + c\dot{x} + kx = 0, \tag{1}$$

or

$$\ddot{x} + \frac{c}{M}\dot{x} + \frac{k}{M}x = 0 \tag{2}$$

In the case of dry friction between the drill 1 and the sliding crossbar 2, the resistive force has a constant magnitude and a value of $F_f = \pm\mu N = \pm\mu G = \pm\mu Mg$ [the (-) sign is taken when the motion occurs in the direction of the axis x]

In this case, equation (2) takes the form:

$$\ddot{x} + \frac{c}{M}\cdot\dot{x} + \mu g = 0 \tag{3}$$

It is assumed that during the drilling process, due to water from the wet drill string, condensate formed in the borehole, and oil particles resulting from leaks in the drill and the feed system motor, there is a permanent film of water-oil mixture in the guides between the drill support plate and the sliding crossbar, a situation in which the free term in equation (3) is neglected, so that the characteristic equation of equation (2) takes the form:

$$\gamma^2 + 2\alpha\gamma + \omega^2 = 0, \tag{4}$$

whose solution is:

$$\gamma_{1,2} = -\alpha \pm \sqrt{\alpha^2 - \omega^2} \tag{5}$$

Let $\alpha^2 - \omega^2 = \beta^2$; from (5) it follows that:

$$\gamma_{1,2} = -\alpha \pm i\beta \tag{6}$$

If $\alpha^2 - \omega^2 < 0$, the roots of the equation are complex conjugates (the case of small friction) and the motion is damped oscillatory.

In this case, the solution to the differential equation, and thus the law of motion, is:

$$x = Ae^{-\alpha t}\cdot\sin(\beta t + \varphi), \tag{7}$$

which can also be written as:

$$x = e^{-\alpha t}\cdot(\mathrm{C}_1\sin\beta t + \mathrm{C}_2\cos\beta t), \tag{8}$$

where $C_1, C_2, A\ and\ \varphi$ are integration constants determined from the boundary conditions and which, in the general case, are: $x = x_0$ and $v = v_0$ for $t = 0$.

For these conditions and for $\alpha^2 < \omega^2$, the law of motion is obtained:

$$x = \sqrt{{x_0}^2 + (\frac{v+\alpha x_0}{\beta})^2}\cdot e^{-\alpha t}\cdot\sin(\beta t + arctg\frac{\beta x_0}{v_0+\alpha x_0}) \tag{9}$$

which represents a damped oscillatory motion.

The amplitude $Ae^{-\alpha t}$ decreases over time, resulting in an amplitude-modulated motion. The quantity β (*pseudo-pulsation*) is given by:

$$\beta = \sqrt{\omega^2 + \alpha^2} = \sqrt{\frac{k}{M} - (\frac{c}{2M})^2} \tag{10}$$

and the period of the pseudo pulsation β is:

$$T_\beta = \frac{2\pi}{\beta} = \frac{2\pi}{\sqrt{\omega^2 + \alpha^2}} \tag{11}$$

b) *the case of damped forced vibrations produced by some perturbing force* (Fig. 2) *in a system with viscous damping* (Fig. 4), this dynamic response occurring during the percussion$(t < t_0)$, when the interaction between the drill bit and rock causes the occurrence of longitudinal oscillations that propagate through the feed system consisting of the sliding crossbar, the traction chain, the gearbox, and the rest of the elements shown in Fig.1)

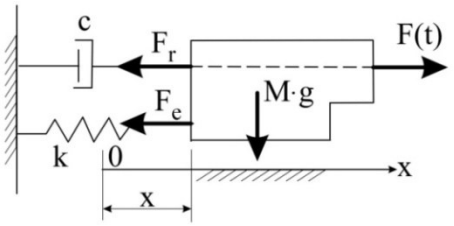

Fig. 4. Viscous dampening vibrations model

In this case, the differential equation of motion takes the form:

$$M\ddot{x} + c\dot{x} + kx = F(t), \tag{12}$$

or

$$\ddot{x} + 2\alpha\dot{x} + \omega x = q_1, \tag{13}$$

where:

$$q_1 = \frac{F(t)}{M}.$$

Equation (13) is a linear differential equation whose solution is of the form:

$$x = x_1 + x_2 \tag{14}$$

The solution x_1 of the homogeneous differential equation is represented by relations (8) and (9), respectively, and represents the natural vibration of the drill-bit-rock system.

The particular solution x_2 of equation (12), i.e., the sustained vibration, is determined using the impulse, assuming that each elementary impulse $q_1 dt$ occurs within the interval $t = 0$ and $t = \tau$, during which an elementary displacement dx occurs, an interval in which the perturbing force is constant, resulting in:

$$x_2 = \frac{1}{\beta} \cdot \int_0^\tau q_1 e^{-\alpha(\tau - t)} \cdot \sin[\beta(\tau - t)dt = \frac{1}{M\beta} \int_0^\tau F(t) e^{-\alpha(\tau - t)} \sin[\beta(\tau - t)dt \tag{15}$$

This integral represents the effect of the perturbing force $F(t)$ over the time interval (0,τ).

The complete solution of the differential equation (13) over the interval (0,τ) becomes:

$$x = e^{-\alpha t} \cdot (\frac{v_0 + \alpha x_0}{\beta} \cdot \sin \beta t + x_0 \cos \beta t) + \frac{1}{M\beta} \int_0^\tau F(t) e^{-\alpha(\tau - t)} \sin[\beta(\tau - t)dt \tag{16}$$

In (16), the first term represents the effect of the initial displacement x_0 and the initial velocity v_0, while the second term represents the effect of the perturbing force $F(t)$.

In the case of the system under study, since $x_0 = v_0 = 0$ at $t = 0$, the law of motion according to relation (16) for t, which belongs to the interval$[0, t]$, becomes:

$$x = \frac{F_0}{M\beta} \int_0^\tau F(t) e^{-\alpha(\tau - t)} \sin[\beta(\tau - t)dt \tag{17}$$

Performing the variable substitution $\tau - t = u$, solving the integral (17) leads to the relation:

$$x = \frac{F_0}{M\beta} \cdot \frac{e^{-\alpha u} (-\alpha \cdot \sin \beta u - \beta \cos \beta u}{\alpha^2 + \beta^2} \Big|_0^\tau \tag{18}$$

Returning to the variable t, we obtain the law of motion:

$$x = \frac{F_0}{M\beta} \frac{e^{-\alpha(\tau - t)} (-\alpha \cdot \sin \beta(\tau - t) - \beta \cos \beta(\tau - t)}{\alpha^2 + \beta^2} \Big|_0^\tau \tag{19}$$

For the upper limit $t = 0$; $\tau \to t$ and for the lower limit $t = \tau$, so $\tau - t = 0$, thus the solution is obtained:

$$x = \frac{F_0}{M\beta(\alpha^2 + \beta^2)} [\beta - e^{-\alpha t} (\alpha \cdot \sin \beta t + \beta \cos \beta t)], \tag{20}$$

for t belonging to the interval $[0, t_0]$.

From (20), the expressions for velocity and acceleration are obtained in the form:

$$v = \dot{x} = \frac{F_0}{M\beta} \cdot e^{-\alpha t} \cdot \sin \beta t \tag{21}$$

$$a = \ddot{x} = \frac{F_0}{M\beta} \cdot e^{-\alpha t} \cdot (-\alpha \cdot \sin \beta t + \beta \cdot \cos \beta t) \tag{22}$$

At the moment the disturbing force ceases, i.e., at $t = t_0$ (Fig. 2), the expressions for displacement, velocity, and acceleration are:

$$x_f = \frac{F_0}{M\beta(\alpha^2 + \beta^2)} [\beta - e^{-\alpha t_0} (\alpha \cdot \sin \beta t_0 + \beta \cos \beta t_0)], \tag{23}$$

$$v_f = \frac{F_0}{M\beta} \cdot e^{-\alpha t_0} \cdot \sin \beta t_0 \tag{24}$$

$$a_f = \frac{F_0}{M\beta} \cdot e^{-\alpha t_0} \cdot (-\alpha \cdot \sin \beta t_0 + \beta \cdot \cos \beta t_0) \tag{25}$$

After the ceasing of the disturbing force ($t > t_0$), the system undergoes damped free vibrations whose initial conditions are given by equations (24) and (25), and the law of motion, according to equation (9), takes the form:

$$x = \sqrt{x_f{}^2 + (\frac{v_f + \alpha x_f}{\beta})^2} \cdot e^{-\alpha t} \cdot \sin(\beta t + arctg \frac{\beta x_f}{v_f + \alpha x_f}) \tag{26}$$

In reality, however, during the drilling process, the disturbing force forms a train of pulses acting on the drill, whose frequency is equal to the frequency of the drill piston's impacts on the drill bit.

Equations (20),(21),(22), and (23),(24),(25) represent the dynamic response of the drill-bit-working tool- rock system, a response that expresses the laws of displacement, velocity, and acceleration during the period ($0, t_0$), when the force F_0 is applied (for the duration of a pulse), and at the end of this period ($t > t_0$).

Results obtained by equipping the system with the P125s drill hammer

The P125 drill hammer (made in Romania) has the following characteristics:

- impact energy: $E = (130 \ldots 160)$J;

- frequency of piston strikes on the drill bit: $f = 2580\ kicks/\text{min}$;
- speed under load: $n = 200\ \text{rot/min}$;
- torque at the drill shaft: $M_t = 45 \ldots 80\ \text{N} \cdot \text{m}$, at $n = 200\ rot/min$ and depending on the supply compressed air pressure

For the study, a hypothetical (but realistic) example was considered, assuming that the drilling speed is $v = 0{,}3\ \text{m/min}$.In this case, the result is:

- a rock penetration rate of $5\text{mm/s}\ and\ 1{,}5\ \text{mm/rot.}$;
- a complete rotation of the drill bit is achieved in 0,3s ;
- a blow frequency of $43\ kicks/\text{s}$

Since the drill bit's kick occurs during rock chipping over the course of one rotation, it follows that in Fig. 2, $t_0 = 1\text{s}$ can be considered.

With the above data, the quantities in equations (20), (21), (22), (23), (24), and (25) have the following values:

- the elastic constant of the oscillating system:

$$k = \frac{Gd^4}{645R^3n} = 371\frac{\text{N}}{\text{mm}},$$

where $G = 8{,}5 \cdot 104\ N/mm^2$,$d = 12\ mm$, $R = 21\ \text{mm}$, $n = 8$

-the square of the amplitude:

$$\omega = \frac{k}{m} = 3905\ [1/s^2\ ]$$

-the damping factor:

$$2\alpha = \frac{c}{m} = 0{,}06 \cdot \sqrt{\frac{k}{m}} = 3{,}7\ [1/s],$$

resulting in the values $\alpha_1 = 1{,}875\ [1/s]$ and $\alpha_2 = 3{,}516\ [1/s^2]$;

-the argument constant of the trigonometric function:

$$\alpha^2 - \omega^2 = -3901^2 = -\beta^2,$$

where $\beta = 3901\ [1/s]$;

-the downforce on the drill bit $F_0 = 7228{,}5\ [\ N\ ]$.

With these values, equations (20)…(26) take the following form:

$$x = \frac{7228{,}5}{95 \cdot 3901(3{,}516^2 + 3901^2)} \cdot [3902 - e^{1{,}875}(1{,}875 \sin 3901t + 3901 \cos 3901t \tag{27}$$

$$v = \dot{x} = \frac{7228{,}5}{95 \cdot 3901} \cdot e^{1{,}875} \cdot \sin 3901t \tag{28}$$

$$a = \ddot{x} = \frac{7228{,}5}{95 \cdot 3901} \cdot (-1{,}875 \cdot \sin 3901t + 3901 \cdot \cos 3901t) \tag{29}$$

$$x_f = \frac{7228{,}5}{95 \cdot 3901(1{,}875^2 + 3901^2)} \cdot [3901 - e^{1{,}875}(1{,}875 \sin 3901t + 3901 \cos 3901t)] = 1{,}95 \cdot 10^{-6} m \tag{30}$$

$$v_f = \dot{x_f} = \frac{7228{,}5}{95 \cdot 3901} \cdot e^{1{,}875} \cdot \sin 3901t = 11{,}6\ [\frac{mm}{s}] \tag{31}$$

$$a_f = \frac{7228{,}5}{95 \cdot 3901} \cdot (-1{,}875 \cdot \sin 3901t + 3901 \cdot \cos 3901t) \tag{32}$$

Figures 5, 6, and 7 show the laws of variation for displacement, velocity, and acceleration for the hypothetical example under consideration.

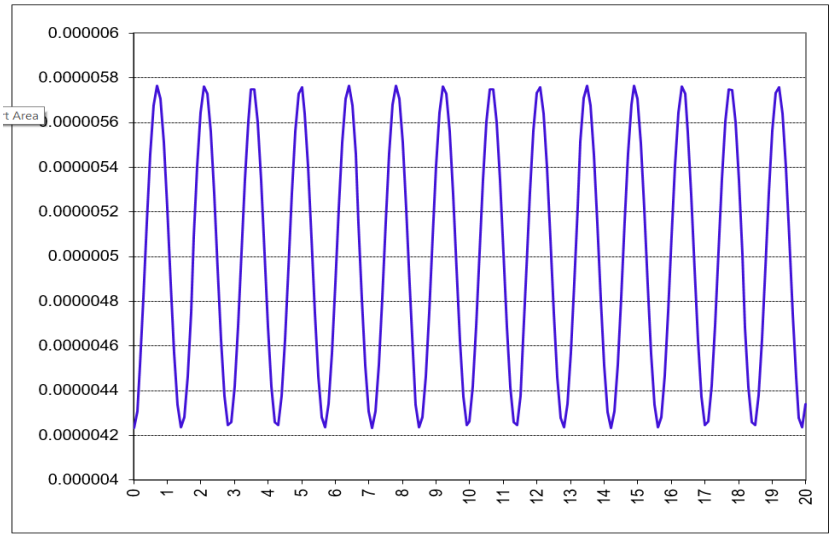

Fig. 5. The displacement variation obtained with P125s drill ($F_f = 0$)

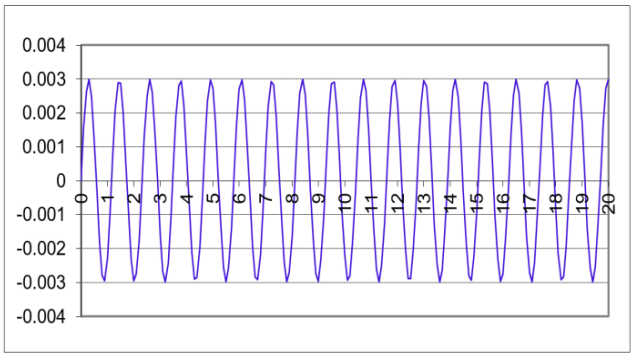

Fig. 6. The velocity variation obtained with P125s drill ($F_f = 0$)

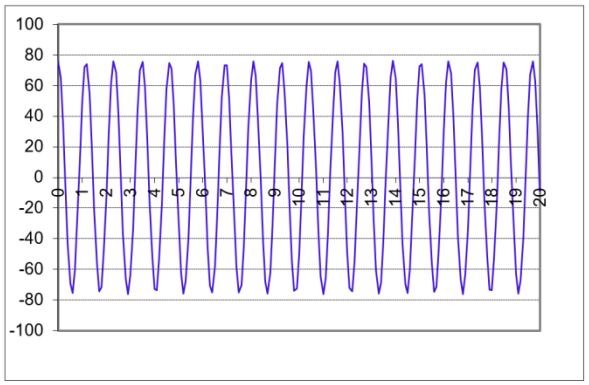

Fig. 7. The acceleration variation obtained with P125s drill ($F_f = 0$)

c) *the case of damped vibrations produced by an arbitrary disturbing force when the friction force in the guides is taken into account*

Next, we will perform a new analysis of the vibration mode of the drill-bit-rock system, in which, this time, we will neglect the damping force in the damper ($F_r = 0$) and take into account the friction force in the guides $F_f = \mu N = \mu G = \mu M g$(Fig. 8).

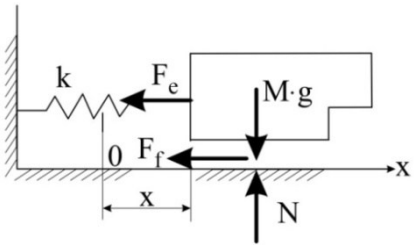

Fig. 8. The vibrations model when the friction force $F_f \neq 0$

If, at the initial moment, the moving mass M is displaced to the right by x_0 due to the force F_0 and, in the interval t_0, it oscillates freely, the differential equation of motion is:

$$Mx + k\ddot{x} = \mu Mg \tag{33}$$

or

$$\ddot{x} + \frac{k}{M} \cdot x = \frac{F_f}{M}; \ddot{x} + \omega^2 \cdot x = \mu g, \tag{34}$$

where $\omega^2 = k / M$.

The solution to equation (34) is:

$$x = A\cos \beta t + B\sin \beta t + \frac{F_f}{k}; 0 \leq \beta t \leq \pi \tag{35}$$

The natural frequency of the vibration is:

$$\omega = \sqrt{\frac{k}{M}},$$

and the particular solution of the differential equation is:

$$x_1 = \frac{\mu y}{\omega^2} = \delta_R \tag{35'}$$

With this value, we obtain the general equations for displacement, velocity, and acceleration:

$$x = Acos\ \omega t + B\sin\omega t + \delta_R \quad (36)$$
$$\dot{x} = -\omega A sin\ \omega t + \omega\beta\cos\omega t \quad (37)$$
$$\ddot{x} = a = -\omega^2(Acos\ \omega t + \beta\sin\omega t) \quad (38)$$

Given the initial conditions $x = x_0$ and $x' = 0$, for $t = 0$ we obtain $B = 0, A = x_0 - \delta_R$, and the equations of displacement, velocity, and acceleration become:

$$x = (x_0 - \delta_R)\cdot\cos\omega t + \delta_R \quad (39)$$
$$v = \dot{x} = -\omega(t_0 - \delta_R\cdot\sin\omega t) \quad (40)$$
$$a = \ddot{x} = \omega^2\cdot\delta_R\cdot\cos\omega \quad (41)$$

The equation of motion is valid for the first half-period, at the end of which $\omega t_1 = \pi$, the displacement being:

$$x_1 = -x_0 + 2\delta_R \quad (42)$$

At the end of the second half-cycle, the moving mass (the kick) will be at the center of oscillation, at a distance of:

$$x_2 = x_0 - 4\delta_R \quad (43)$$

The moving mass M continues its motion as long as the driving force is greater than the resisting force. It stops after a number y of half-cycles for which:

$$k(x_0 - 2y\delta_R) \leq \mu Mg, \quad (44)$$

from which it follows that y .

For the numerical example of calculating this mode of vibration, we will use the following data: $M = 99{,}5\ kg$; $k = 371\ N/mm$; $\mu = 0{,}1$; $x_0 = 1{,}5\ mm$; $\omega = 62{,}49\ [1/s]$; $\delta_R = 0{,}2512\ mm$.

With the above values of the quantities involved in the equation of motion, velocity, and acceleration, these become:

$$\left.\begin{aligned} x &= 1{,}2488\cdot\cos 62{,}49t + 0{,}2512\ [m] \\ v = \dot{x} &= -73{,}037\cdot\sin 62{,}49t\ \left[\frac{m}{s}\right] \\ a = \ddot{x} &= -464{,}08\cdot\cos 62{,}49t\ [\frac{m}{s^2}] \end{aligned}\right\} \quad (45)$$

Fig. 9, Fig. 10, and Fig. 11 show the variations of the quantities x , x' , x'' (displacement, velocity and acceleration), given by relations (45).

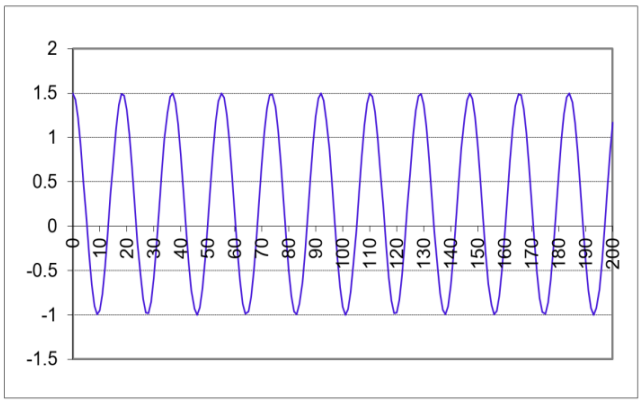

Fig. 9. Displacement variation obtained with P125s drill ($F_f \neq 0$)

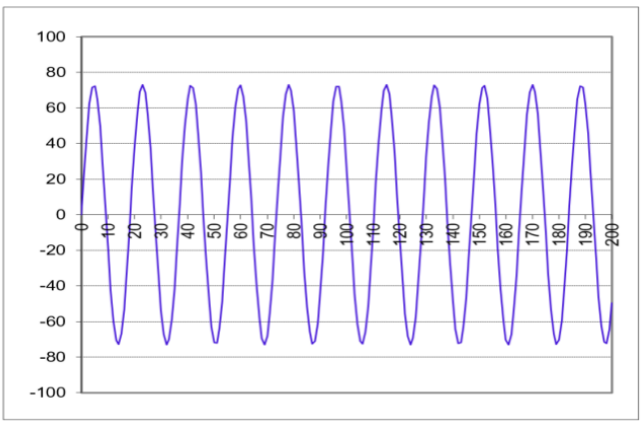

Fig. 10. Velocity variation obtained with P125s drill ($F_f \neq 0$)

Fig. 11. Acceleration variation obtained with P125s drill ($F_f \neq 0$)

To complete the study using purely analytical methods, after determining the dynamic response in terms of displacements, the inertia force is calculated and then introduced into the force system together with the disturbing force (impact force) and the permanent forces (the weights of the elements comprising the feed system, the reactions, and the friction forces).

Using the principle of superposition of effects, the maximum and minimum forces are determined, with which the stresses and then the strains in the structural elements of the oscillating system (the advance system of the drilling rig) are calculated. However, since the stresses are variable, the vibration resistance checks are reduced to determining a safety factor for the normal and tangential stresses.

We will, however, use the results obtained analytically for the considered vibration modes for the finite element modeling of the drill-bit-rock system, but not before making the following preliminary observations:

-the stress in the chain of elements forming the drill hammer's drive mechanism during the active phase (the percussion) depends largely on the hammer's vibration mode;

-Fig. 5 shows that the system's damping is relatively high

-due to the mass (high inertia), oscillations are quickly damped in the sliding crossbeam and the front clamping cylinder, so that they can be neglected in the vibration analysis; the critical element of the feed system (from a vibration standpoint) is the chain with plate-links and rollers that guides the drill bit at the face, where stresses may occur that could lead to its breakage.

2.2. Numerical modeling using the finite element method of the drill-working tool-rock system

In the model proposed for analysis with finite element, the vibrations in the sliding crossbeam and the front hydraulic clamping cylinder were neglected, which, as specified above, have a high damping factor (the vibrations dampen quickly)

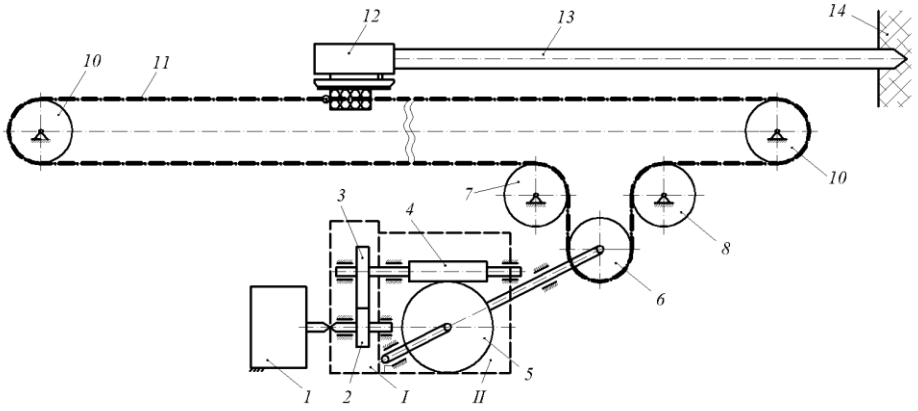

Fig. 12. The simplified kinematic diagram of the working tool assembly

Fig. 12 shows the simplified kinematic diagram of the movement mechanism of the P-125s drill, which is used in IMP-1 and IMP-2 drilling rigs; this diagram includes the drill-working tool-rock wall system that is the subject of this paper. In Fig 12, the following are labeled: 1—pneumatic drive motor; I+II—feed mechanism consisting of a two-stage reducer (a cylindrical gear I and a worm gear-worm wheel II); 2, 3—cylindrical gear wheels;4, 5—the worm gear and the worm wheel, respectively; 6—drive sprocket; 7, 8—chain deflection sprockets; 9, 10—chain return sprockets; 11—traction chain (working element); 12—drill; 13—drill bit; 14—rock wall being drilled.

The main parameters and characteristics of the hammer-bit system are as follows: $M = 99.4\,kg$ – mass of the hammer assembly, $E = 140 - 165\,J$ – impact energy of the piston, $f = 2400 - 2550\,kicks/min$ – frequency of piston strikes on the hammer-bit, $l(s) = 3320mm$—drill bit length, $M_s = 21.5\,kg$—mass of the shank-sleeve-drill bit-cutting crown assembly, $A_s = 804\,mm^2$ -cross-sectional area of the drill bit, for a diameter $d_s = 32\,mm$, $M_l = 3.85\,kg/m$—mass per linear meter of the chain, $A_l^{min} = 252\,mm^2$ -minimum cross-sectional area of the chain, $p_l = 31.75\,mm$-chain pitch.

The modeling of the drill-working tool-rock assembly is shown in Fig. 13, where the following symbols are used: 1 – drill, 2 – working tool, 3 – drill bit, 4 – rock, 5 – friction element. The entire assembly was discretized into 3,204 elements of types BEAM 3D, SHELL 3, GAP, and MASS, via 1,684 nodes, resulting in a system of 10,092 equations. To simplify the modeling, the rock block 4 was assumed to be parallelepiped in shape, with all sides measuring 4 m.

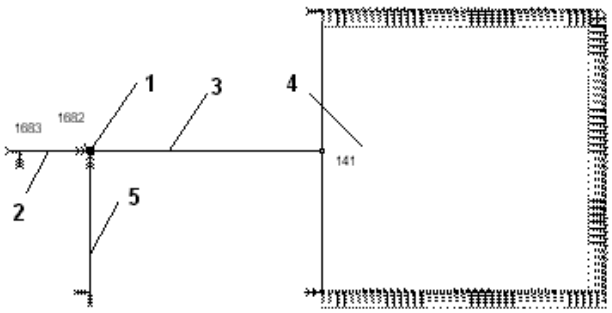

Fig. 13. The F.E.M. model for the drill-working tool-rock system

In the hypothetical calculation example, the following characteristics were assumed for the rock: $E = 70 \times 10^6 N/mm^2$, $r = 2.34 \times 10^3 kg/m^3$.

Drill bit 3 has the following characteristics: length $l = 3320\,mm$, diameter $d = 32\,mm$, contact area between the drill bit crown teeth and the rock $A = 40\,mm^2$, modulus of elasticity $E = 21 \times 10^{10} N/m^2$, length $l = 1\,m$.

The study was conducted over the duration of three consecutive kicks of the piston on the drill bit head.

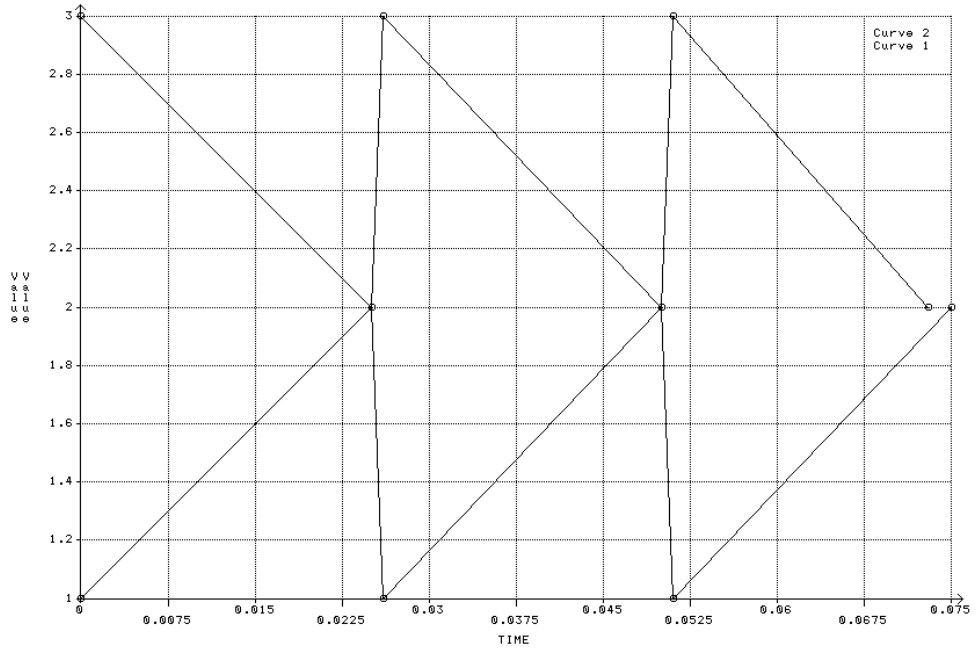

Fig. 14. Force amplification coefficient variation

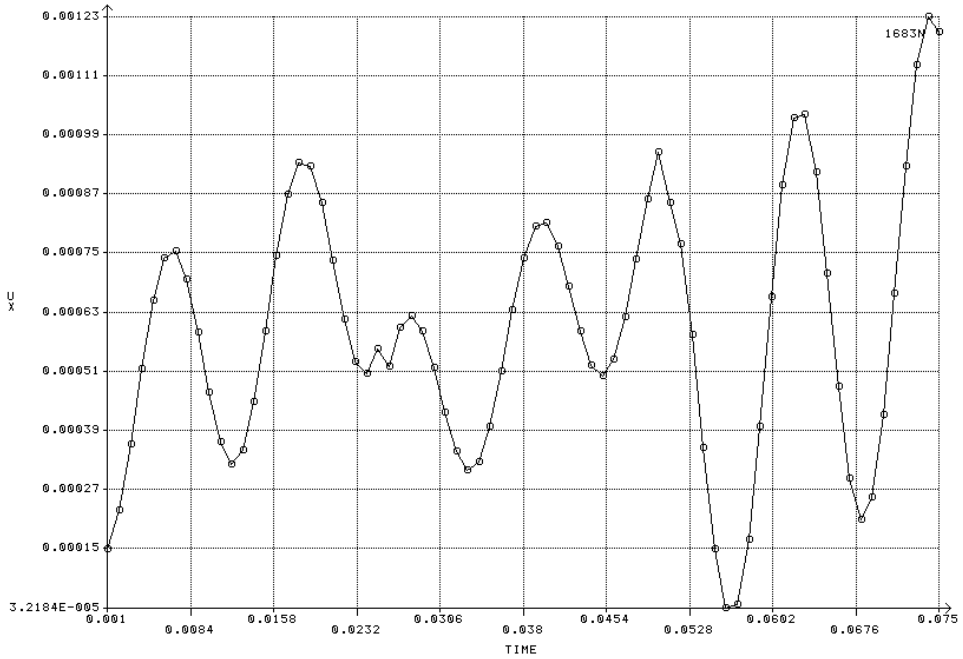

Fig. 15. Displacement diagram for node 1683

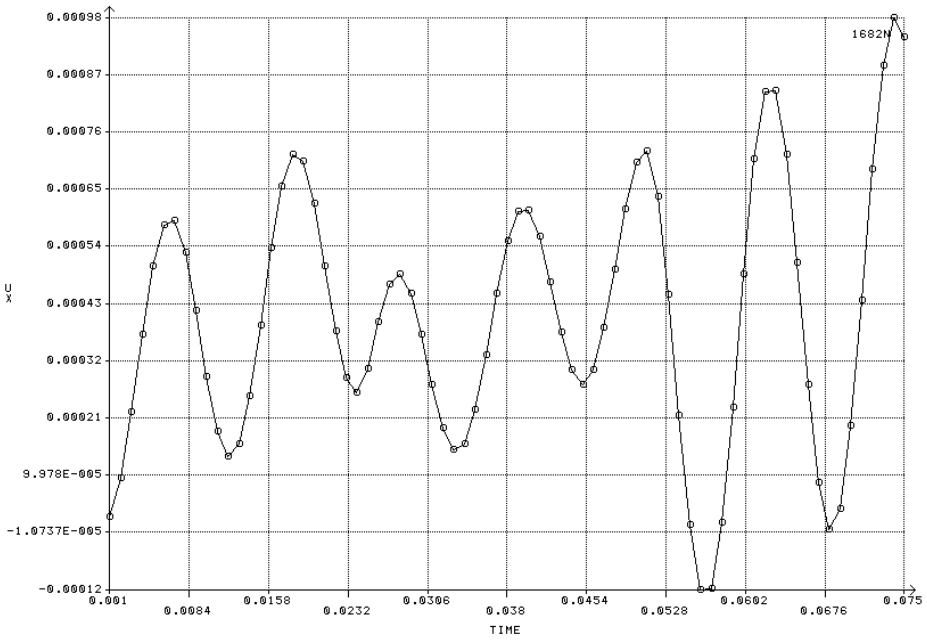

Fig. 16. Displacement diagram for node 1682

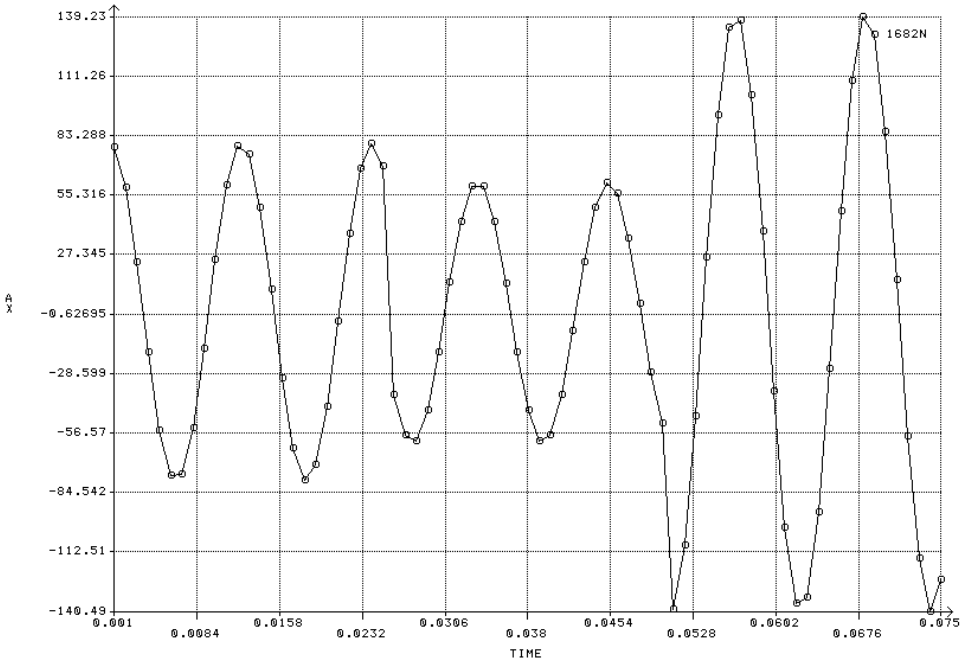

Fig. 17. Acceleration diagram for node 1682

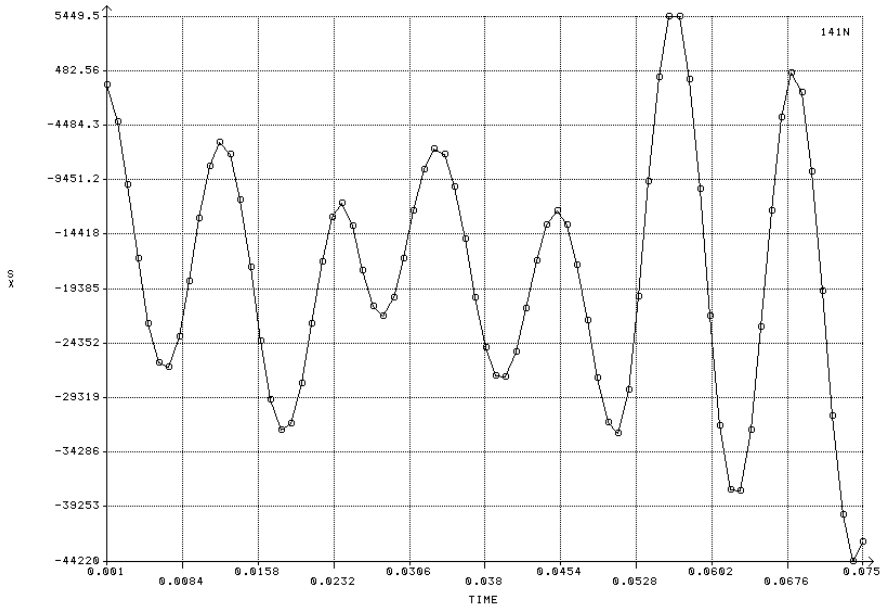

Fig. 18. Rock stress variation for the duration of three consecutive kicks

Results obtained with the numerical modelation:

Figure 14 shows the variation over time of the force amplification coefficient (dynamic multiplier) at nodes 1682 and 1683, for a kicking frequency of the drill piston on the drill bit of f = 2400 kicks/min.

Following the dynamic analysis using the finite element program, for the presented model (Fig. 13), the variation curves of the displacement of the working element's end (node 1683, Fig. 15), as well as the displacement and acceleration of the drill hammer (node 1682, Fig. 16 and Fig. 17) where presented. The rock stress variation resulted during the time of the applied kicks is also presented in Fig. 18. Prior knowledge of rock stresses helps with the optimization of the drill hammer's operating conditions, so as to achieve the best possible drilling speed.

3. Conclusions

Following the modeling of the assembly and the calculations performed, the variation of displacements in the working element of the drill bit as well as the variation of rock stress along the drill bit axis were highlighted for the hypothetical example considered. The results obtained through FEM modeling of the drill-working tool-rock system agree with those obtained analytically, with errors falling within acceptable limits, which confirms the correctness of the chosen model.

The results obtained using the model presented in this paper can be further utilized, for example, to verify the strength of the chain with link-plates and rollers that move the drill bit at the face, for its most unfavorable stress case, namely when the drill bit becomes stuck in the rock and, to unblock (remove) it, the front-mounted locking cylinder of the sliding crossbeam is actuated instead of the drill's movement mechanism. Experience has shown that a dangerous load can occur in the traction chain as a result of the sudden application of the drill bit release force, which may exceed the breaking strength for which the chain was designed (as specified by the manufacturer), which requires special attention from the drilling rig operator.

References

1. Mária Bali Hudáková, Edita Lazarová, Víťazoslav Krúpa, Lucia Ivaničová, Pavol Vavrek, Alexander Kiovský, Analysis in Process Parameters in Rotary Drilling in Andesite. Lipiec - Grudzień 2025 July - December – Journal of the Polish Mineral Engineering Society
2. S.Kahraman, N.Bilgin, C.Feridunoglu, "Dominant rock properties affecting the penetration rate of percussive drills", International Journal of Rock Mechanics and Mining Sciences 40, 711–723 (2003).
3. V. Krúpa, M. Kruľáková, E. Lazarová, M. Labaš, K. Feriančiková, L. Ivaničová, "Measurement, modeling and prediction of penetration depth in rotary drilling of rocks", Measurement: Journal of the International Measurement Confederation 117, 165–175(2018).
4. F.E. Dupriest and W.L. Koederitz, "Maximizing Drill Rates with Real-Time Surveillance of Mechanical Specific Energy", in SPE/IADC Drilling Conference-2005, edited by Society of Petroleum Engineers, Amsterdam, Netherlands, pp.10.
5. Lazarová, E., Kruľáková, M., Krúpa, V., Ivaničová, L. (2014). Determination of Rock Cutting Conditions by Specific Energy., Proceedings IOC 2014, Grafomed-Trade, Serbia, p. 220–223.
6. Krúpa, V., Lazarová, E. (2004). Three rock strength characteristics of Branisko rock mass. Proceeding Geotechnika - 2004 - Geotechnics, Orgware Stupava, Slovakia, p. 271–275.
7. Krúpa, V., Lazarová, E., Ivanicová, L. , Krulaková, M. , Ferianciková, K., Labas, M. Assessment of the Efficiency of the Applied TBM Excavation Regime Inżynieria mineralna — Styczeń – Czerwiec (2015) January – June — Journal of the Polish Mineral Engineering